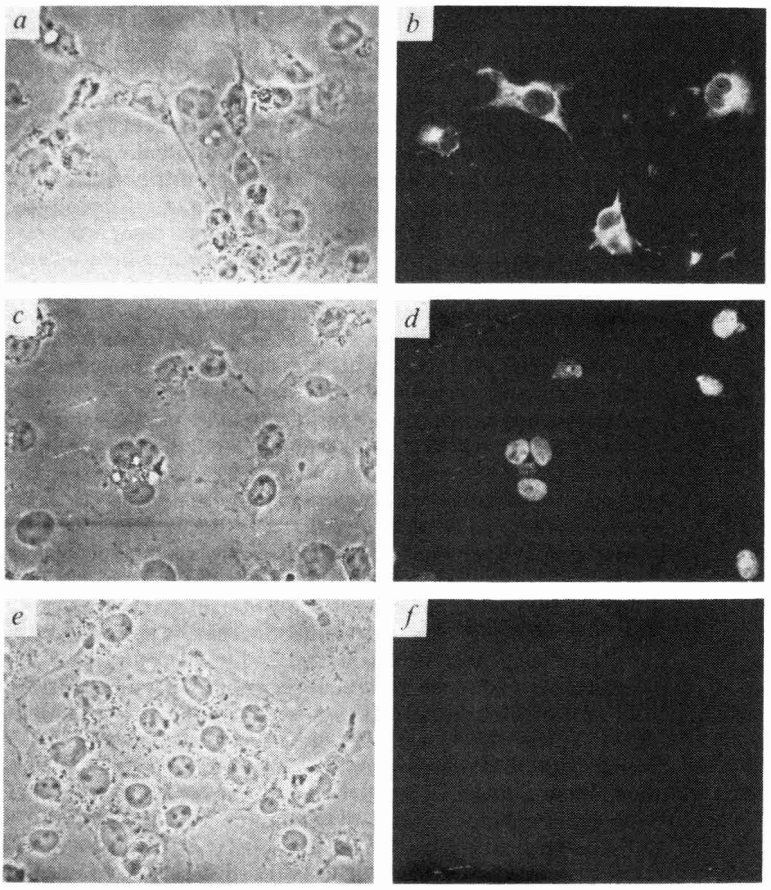

FIG. 3 Subcellular localization of Int-2 proteins by indirec immunofluorescence. The panels show phase contrast (*a*, and *e*) and corresponding fluorescence (*b*, *d* and *f*) micro graphs of COS-1 cells transfected with KC4.3 (*a* and *b* KC4.2 (*c* and *d*), and KC4 (*e* and *f*). KC4.3 and KC4.2 ar equivalents of the constructs depicted in Fig. 2*a*, but withou the Q-65 mutation in the glycosylation site.
METHODS. COS-1 cells were transfected with plasmids KC4 KC4.3 and KC4.2 by electroporation, grown on glass cover slips, and 60 h later fixed in 3% paraformaldehyde in PBS and permeabilized in 0.2% Triton X-100 in PBS. After pre incubation in 1% BSA for 5 min, the coverslips were exposed to a 1:200 dilution of affinity-purified antiserum against a C-terminal Int-2 peptide for 30 min at room temperature. Immune complexes were detected with a rhodamine-conjugated gamma globulin fraction of porcine anti-rabbit serum (Dako Pats) and visualized by fluorescence microscopy using a Zeiss Axiophot microscope.

N-terminally extended forms of human basic FGF that are initiated at any of three alternative CUG codons have recently been described[21,22]. It will be interesting to determine their subcellular fate, because the additional sequences are similarly rich in arginine and proline. A nuclear location for basic FGF has indeed been reported, but in cells responding to, rather than producing, the factor, and predominantly in the nucleolus[23]. There could be an analogous situation for Int-2, because in some of the cells expressing the CUG-initiated product, the staining was distinctly concentrated in the nucleolus. In others, a punctate pattern was observed. The reasons for this variability remain to be determined, but results could be influenced by the physiological state of individual cells or their position in the cell cycle.

There are precedents for the localization of proteins to both the nucleus and secretory pathway. For example, in cells expressing v-*sis*, PDGF-related antigens are detectable in the nucleus[24], and the proportion of the nuclear forms is increased by mutations in the v-Sis signal peptide[25]. More significantly, the rat prostatic protein, probasin, shows dual localization as a result of the use of alternative initiation codons[26]. In contrast to Int-2, the synthesis of a nuclear form of probasin is initiated at an internal AUG codon downstream of the sequence encoding the signal sequence.

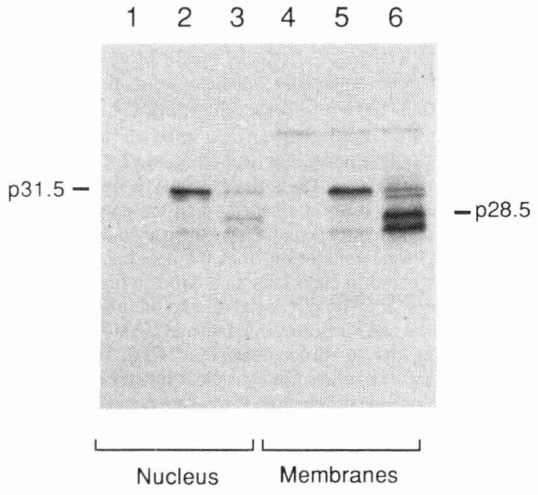

FIG. 4 Subcellular partitioning of Int-2 proteins. Immunoblot of nuclear (lanes 1, 2 and 3) and membrane (lanes 4, 5 and 6) fractions from COS-1 cells transfected with the KC4 vector (lanes 1 and 4), KC4.2Q (lanes 2 and 5) and KC4.3Q (lanes 3 and 6). The main CUG-initiated product from KC4.2Q, p31.5, is predominantly nuclear, although appreciable amounts are contained in the membrane fraction. The main AUG-initiated products, p28.5 and p27.5, seem to be localized predominantly in the membrane fraction. The smaller products expressed from KC4.2Q are interpreted as deriving from residual initiation at the mutated codon, and a small amount of product resulting from signal-peptide cleavage of p31.5.
METHODS. COS-1 cells transfected with the appropriate plasmids were collected 60 h later and lysed in 5–8 volumes of hypotonic buffer containing 2 mM $NaHCO_3$, 1 mM $MgCl_2$, 1 mM EDTA and protease inhibitors. After disruption with a Dounce homogenizer, the cell extract was centrifuged at 800*g* for 10 min to recover a crude nuclear pellet. The supernatant was centrifuged at 130,000*g* for 1 h to obtain a mixed mitochondrial and microsomal pellet. The latter was rinsed in HS buffer (10 mM HEPES buffer, pH 7.4, 0.25 M sucrose, 3 mM $MgCl_2$, and protease inhibitors) containing 0.15 M KCl, and collected by centrifugation. The nuclear pellet was further purified by washing twice in HS buffer, and three times in 10 volumes of 10 mM Tris-HCl buffer, pH 7.4, 1 mM EDTA, 2 mM $MgCl_2$ and 0.25 M sucrose (TESM). The pellet, recovered by centrifugation at 800*g*, was resuspended in 40% (w/w) sucrose in 10 mM Tris-HCl buffer, pH 7.4, and 1 mM $MgCl_2$, and centrifuged through a cushion of 61.5% (w/w) sucrose at 80,000*g* for 2 h. This purified nuclear pellet was finally washed twice in TESM containing 2% CHAPS to remove residual nulcear envelope, and collected by centrifugation. All manipulations were performed in the cold. Equivalent aliquots of each cell fraction were analysed by SDS-PAGE in a 12.5% gel and Int-2-related proteins were detected by immunoblotting as described previously (Fig. 2, and ref. 11).

The data presented here could indicate a dual function for nt-2 in influencing cell behaviour. The AUG-initiated protein as the hallmarks of an extracellular signalling factor and could e destined for a predominantly paracrine role, whereas the UG-initiated product is more likely to have an autocrine ffect on cells that are expressing *int-2*. Finding whether this ffect is positive or negative, or whether it influences the growth r differentiation of the cell, should provide important insights nto the contribution of Int-2 during embryogenesis and umorigenesis. □

ceived 29 September; accepted 18 December 1989.

1. Gospodarowicz, D., Ferrar, N., Schweigerer, L. & Neufeld, G. *Endocrine Reviews* **8,** 95–114 (1987).
2. Rifkin, D. B. & Moscatelli, D. *J. cell. Biol.* **109,** 1–6 (1989).
3. Dickson, C. & Peters, G. *Nature* **326,** 833 (1987).
4. Dickson, C., Smith, R., Brookes, S. & Peters, G. *Cell* **37,** 529–536 (1984).
5. Peters, G. & Dickson, C. in *Cellular and Molecular Biology of Mammary Cancer* eds D. Medina *et al.* 307–319 (Plenum, New York, 1987).
6. Wilkinson, D. G., Peters, G., Dickson, C. & McMahon, A. P. *EMBO J.* **7,** 691–695 (1988).
7. Wilkinson, D. G., Bhatt, S. & McMahon, A. P. *Development* **105,** 131–136 (1989).
8. Moore, R. *et al. EMBO J.* **5,** 919–924 (1986).
9. Smith, R., Peters, G. & Dickson, C. *EMBO J.* **7,** 1013–1022 (1988).
10. Mansour, S. L. & Martin, G. R. *EMBO J.* **7,** 2035–2041 (1988).
11. Dixon, M. *et al. Molec. cell. Biol.* **9,** 4896–4902 (1989).
12. Hann, S. R., King, M. W., Bentley, D. L., Anderson, C. W. & Eisenman, R. N. *Cell* **52,** 185–195 (1988).
13. Peabody, D. S. *J. biol. Chem.* **264,** 5031–5035 (1989).
14. Yoshida, T. *et al. Proc. nant. Acad. Sci. U.S.A.* **84,** 7305–7309 (1987).
15. Delli-Bovi, P. *et al. Molec. cell. Biol.* **8,** 2933–2941 (1988).
16. Zhan, X., Bates, B., Hu, X. & Goldfarb, M. *Molec. cell. Biol.* **8,** 3487–3495 (1988).
17. Harlow, E., Crawford, L. V., Pim, D. C. & Williamson, N. M. *J. Virol.* **39,** 861–869 (1981).
18. Hortsch, M. & Meyer, D. *Eur. J. Biochem.* **150,** 559–564 (1985).
19. Dingwall, C. & Laskey, R. A. *A. Rev. Cell Biol.* **2,** 367–390 (1986).
20. Brookes, S., Smith, R., Casey, G., Dickson, C. & Peters, G. *Oncogene* **4,** 429–436 (1989).
21. Prats, H. *et al. Proc. natn. Acad. Sci. U.S.A.* **86,** 1836–1840 (1989).
22. Florkiewicz, R. Z. & Sommer, A. *Proc. natn. Acad. Sci. U.S.A.* **86,** 3978–3981 (1989).
23. Bouche, G. *et al. Proc. natn. Acad. Sci. U.S.A.* **84,** 6770–6774 (1987).
24. Yeh, H.-J., Pierce, G. F. & Deuel, T. F. *Proc. natn. Acad. Sci. U.S.A.* **84,** 2317–2321 (1987).
25. Lee, B. A., Maher, D. W., Hannink, M. & Donoghue, D. J. *Molec. cell. Biol.* **7,** 3527–3537 (1987).
26. Spence, A. M. *et al. Proc. natn. Acad. Sci. U.S.A.* **86,** 7843–7847 (1989).
27. Kozak, M. *J. Cell Biol.* **108,** 229–241 (1989).

ACKNOWLEDGEMENTS. We thank Francis Fuller-Pace and John Armstrong for discussions, Roger Watson and Gerard Evan for comments on the manuscripts, David MacAllan, John Armstrong and Ed Harlow for anti-peptide Int-2 serum, anti-docking protein serum and anti-T antigen antibodies, respectively, and Iain Goldsmith for the preparation of synthetic oligonucleotides.

Retinoblastoma in transgenic mice

Jolene J. Windle*, Daniel M. Albert†, Joan M. O'Brien†, Dennis M. Marcus†, Christine M. Disteche‡, Rene Bernards§ & Pamela L. Mellon*‖

* Regulatory Biology Laboratory, The Salk Institute for Biological Studies, 10010 North Torrey Pines Road, La Jolla, California 92037, USA
† Howe Laboratory of Ophthalmology, Massachusetts Eye and Ear Infirmary, Harvard Medical School, 243 Charles Street, Boston, Massachusetts 02114, USA
‡ Department of Pathology, University of Washington, School of Medicine, Seattle, Washington 98195, USA
§ Massachusetts General Hospital Cancer Center, Harvard Medical School, Bldg. 149 13th Street, Charlestown, Massachusetts 02129, USA

RETINOBLASTOMA, a malignancy of the eye occurring in young children, has been widely studied as a model for genetic predisposition to cancer. This disease is caused by mutations in both alleles of an anti-oncogene (the retinoblastoma gene, *Rb*) that inactivate or eliminate the *Rb* encoded protein, p105^{Rb} (refs 1 and 2). Here we report that expression of a viral oncogene, the simian virus 40 T antigen, in the retina of transgenic mice produces heritable ocular tumours with histological, ultrastructural and immunohistochemical features identical to those of human retinoblastoma. Furthermore, we demonstrate a specific association[3] between p105^{Rb} and T antigen in mouse retinoblastoma tumour cells. Thus, the occurrence of these tumours is *in vivo* evidence for oncogenesis due to the ocular-specific expression of an Rb-binding oncoprotein that can functionally inactivate the Rb protein. As an animal model for heritable retinoblastoma, these mice should allow the study of the ontogeny, pathogenesis and treatment of this malignant disease.

Fifteen lines of transgenic mice were derived from fertilized ova microinjected with a chimaeric gene containing the protein coding region of the simian virus 40 (SV40) T antigen (*Tag*) driven by the promoter of the luteinizing hormone β-subunit gene (*LHβ*)[4]. The introduction of *Tag* into transgenic mice has produced tumours of a variety of tissues[5,6], both by directed oncogenesis[7–9] and by ectopic expression[10]. The *LHβ-Tag* hybrid gene directed a low level of *Tag* expression specifically to gonadotrope cells of the anterior pituitary in most of the lines of mice, but did not result in observable histological abnormalities in this organ until 10–12 months of age. However, a single male founder developed bilateral ocular neoplasms at about 5 months of age. The phenotype was heritable with complete penetrance in transgenic offspring. Retinal tumours were first observed at about 2 months of age, and filled the vitreous cavity by 5–6 months of age.

A variety of tissues from this line of transgenic mice, including ocular tumours, were assayed for *Tag* messenger RNA by northern blotting. *Tag* mRNA was present at marginally detectable levels in the pituitary, and at considerably higher levels in the eye, with the level increasing as the tumours developed (Fig. 1). *Tag* mRNA was absent from other tissues.

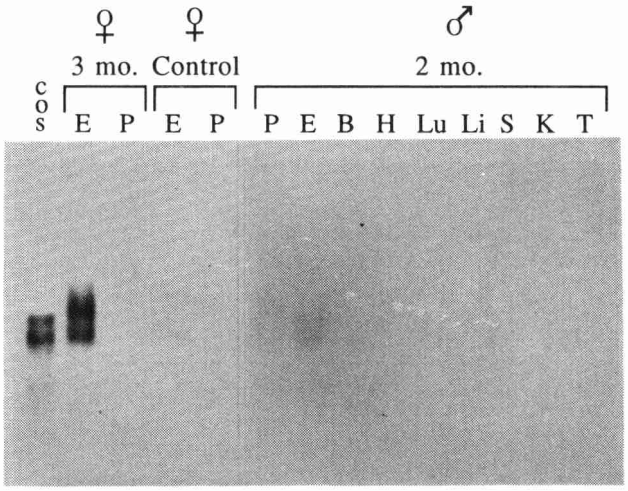

FIG. 1 SV40 *Tag* expression in various tissues of *Tag Rb* mice. Total RNA was prepared as described[30] from the eye and pituitary of a 3-month-old transgenic female in which development of ocular tumours was readily apparent, and from various tissues of a 2-month-old transgenic male in which the presence of an ocular tumour was only apparent on histological examination. In addition, RNA was prepared from the eye and pituitary of a nontransgenic control female and from COS cells, which constitutively express *Tag*[31]. *Tag* mRNA levels were assayed by northern analysis[32], using a probe specific for *Tag* (SP6TagHB, provided by Y. Gluzman). Total RNA (10 μg) was present in each lane, except for the pituitary samples, which contained either 5.0 μg (the transgenic and control females) or 7.6 μg (the transgenic male). Abbreviations: E, eye; P, pituitary; B, brain; H, heart; Lu, lung; Li, liver; S, spleen; K, kidney; T, testes; mo, months.
METHODS. The *LHβ-Tag* transgene contains the human LH β-subunit promoter region[4] from −1.09 kilobases to +9 base pairs linked to the SV40 early region from the *Bgl*I site to the *Bam*HI site[33]. This fragment contains the coding region for Tag and small t antigen, including the translation initiation and transcription termination sites, but lacks the SV40 early promoter. The hybrid gene was precisely excised from the plasmid vector, purified and injected into fertilized one-cell embryos essentially as described[34]. The F_2 embryos were derived from matings of CB6F1/J (C57Bl/6J×BALB/cJ) males and females, obtained from the Jackson Laboratory.

‖ To whom correspondence should be addressed.

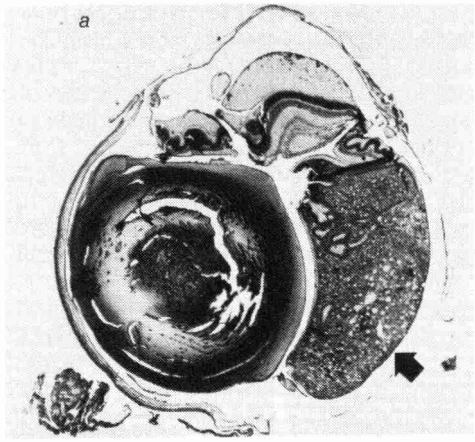
a

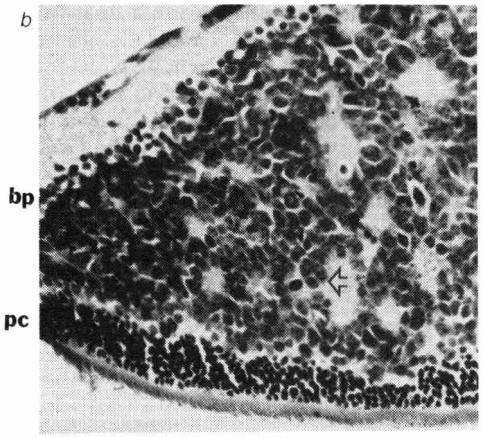
b
bp
pc

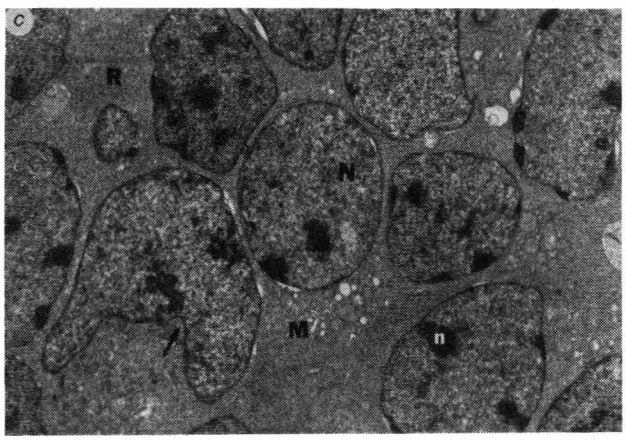
c
R
N
M
n

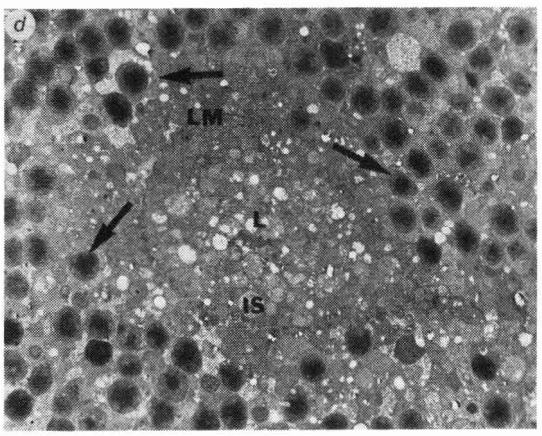
d
LM
L
IS

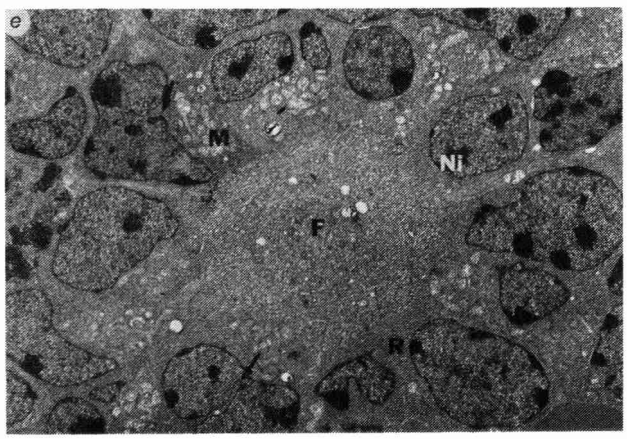
e
M
Ni
F
R

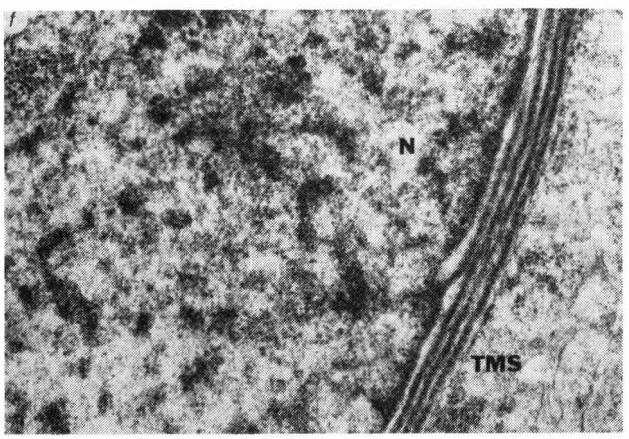
f
N
TMS

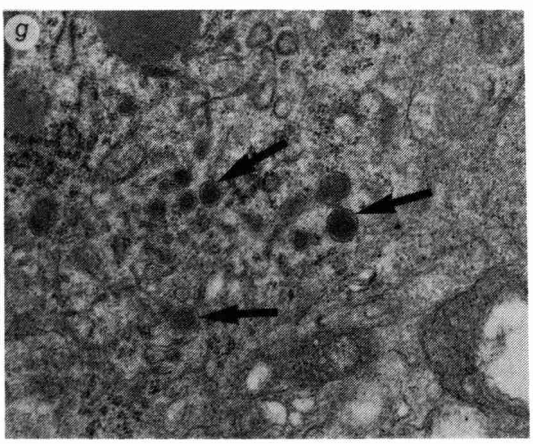
g

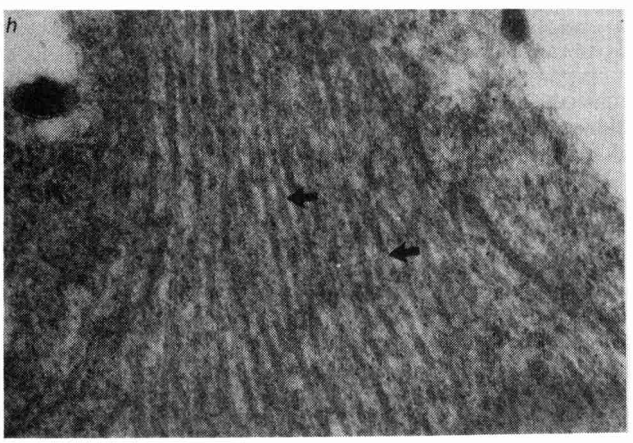
h

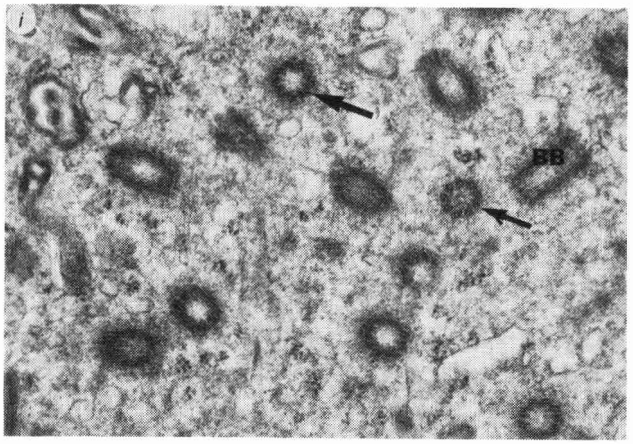

FIG. 2 Light and transmission electron microscopy of ocular tumour sections. Eyes were enucleated at about 5 months of age. The globes were fixed in 5% buffered formalin or 3% phosphate buffered glutaraldehyde–sucrose and processed for light (*a*, *b*) or transmission electron microscopy (*c*–*i*), respectively. *a*, Low-power view of eye containing retinoblastoma (arrow). *b*, Haematoxylin and eosin stain of retinoblastoma cells (arrow) interposed between the bipolar cell layer (BP) and photoreceptor cells (PC). The tumour is composed of both undifferentiated cells and rosettes. Magnification, ×350. *c*, Area of tumour cells similar in appearance to undifferentiated tumour cells found in human retinoblastoma. The cells have prominent round nuclei (N), multiple nucleoli (n), and in some cases indentations of nuclear membrane (arrow). The cytoplasm is relatively scanty and contains ribosomes (R) and mitochondria (M). Magnification, ×9,150. *d*, Highly differentiated rosette composed of photoreceptor-like cells (arrows) having similarity to Flexner–Wintersteiner rosette. Delicate limiting membrane (LM) is present. Disorganized inner segment material (IS) fills lumen (L). Magnification, ×630. *e*, Cuboidal cells forming a rosette configuration around a fibrous matrix (F) resembling a Homer Wright rosette. Nuclei contain multiple nucleoli (Ni), fine marginal chromatin, and occasional indentations of nuclear surface (arrows). Mitochondria (M) and aggregates of ribosomes (R) are present in the cytoplasm. Magnification, ×3,400. *f*, Nuclear membrane of mouse tumour cells shows triple membrane structure (TMS) with dense chromatin-like material associated with the nuclear membrane. The Figure includes a portion of the nucleus (N). Magnification, ×18,000. *g*, Neurosecretory granules (arrows) in mouse retinoblastoma cell cytoplasm, measuring 900–1,100 Å in diameter. These granules are frequently seen in human retinoblastoma cells and in the amacrine cells of the retina. Magnification, ×22,440. *h*, Microtubules (arrows) in the cytoplasm of mouse tumour cells, measuring 200–250 Å in diameter. Magnification, ×42,750. *i*, Transverse sections of cilia with a pattern of 9+0 microtubules (arrows) in mouse tumour cell cytoplasm. Similar cilia occur in human retinoblastoma cells as well as photoreceptor cells. Basal bodies (BB) are also present. Magnification, ×9,920.

The histology of retinoblastoma is well described[11,12], and the features of this malignancy were closely paralleled by the murine tumours (Fig. 2*a*). Human retinoblastoma is a small cell tumour of the sensory retina. The predominant cell type has a large hyperchromatic nucleus with minimal cytoplasm. These poorly differentiated cells have a high mitotic index and may be precursors of more-differentiated tumour cells displaying features of photoreceptor cells. Perivascular cuffs of viable tumour cells surround retinal vessels and contrast prominently with areas of necrosis and calcification near these vessels[13]. These features were observed in the murine tumours both by light microscopy (Fig. 2*b*) and by electron microscopy (Fig. 2*c*).

Human retinoblastoma cells undergo photoreceptor cell differentiation to form characteristic rosettes, first described by Flexner[14] and Wintersteiner[15]. These rosettes are composed of cuboidal cells attached at apical ends to terminal bars, which surround a central lumen and are uniquely associated with retinoblastoma. A second structure, the Homer Wright rosette, is composed of a single row of less-differentiated cells arranged in a radial pattern around a tangle of fibrous cytoplasmic processes[16]. Rosettes of both types were observed by light and electron microscopy in every transgenic mouse tumour examined (Flexner–Wintersteiner rosettes are shown in Fig. 2*b* and *d*, and Homer Wright rosettes are shown in Fig. 2*b* and *e*).

Ultrastructural studies of the murine tumours revealed additional features that are characteristic of human retinoblastoma. Lamelliform nuclear membranes, in which a central dense layer of either granular or fibrillar chromatin is bounded on both sides by membrane, were often observed. Neurosecretory granules, cytoplasmic microtubules, and cilia with a '9+0' pattern of microtubules in which the shafts lack central processes, were also observed (Fig. 2; *f*, *g*, *h* and *i*, respectively). These ultrastructural features are characteristic of human photoreceptor cells and of both human and murine retinoblastoma cells differentiating along the photoreceptor cell lineage.

Immunohistological staining for neuron-associated antigens in tumours from transgenic mice also provided results consistent with those obtained from human retinoblastoma. Kyritsis and colleagues demonstrated[17] both neuron specific enolase (NSE) and glial fibrillary acidic protein (GFAP) in undifferentiated human retinoblastoma cells. With differentiation, retinoblastoma cells showing glial morphology become negative for NSE, whereas those with neural features become negative for GFAP[17]. The transgenic murine tumours stained positively for NSE and negatively for S-100 and vimentin. GFAP was identified in the supporting stroma of the tumour but not in the tumour itself. These immunohistochemical features are consistent with a neural pattern of differentiation and are identical to the staining pattern of the well characterized human retinoblastoma cell line Y-79 (ref. 18; data not shown).

In the eye, malignant extension of human retinoblastoma occurs by local invasion or by vitreous seeding[11,12]. Endophytic tumours grow from the inner retina into the vitreous cavity. Exophytic tumours extend towards the choroid and produce retinal detachment; these tumours can eventually extend along ciliary vessels and nerves to the orbit. Invasion of the optic nerve with malignant extension to the brain also occurs[11,12]. Endophytic and exophytic growth are most commonly observed in the same eye. Transgenic murine tumours displayed both endophytic and exophytic growth, with invasion of retina and choroid, vitreous seeding and optic nerve invasion. These tumours arose bilaterally, with several foci, as occurs in heritable human retinoblastoma.

The remarkable fidelity with which the retinal tumours in these mice displayed the highly specific and complex ultrastructural features of human retinoblastoma, indicates that there may be a common underlying mechanism for tumorigenesis at the molecular level. One possibility is that the *Rb* locus was disrupted by the transgene or suffered some other mutation, and tumorigenesis resulted from a frequent somatic mutation of the second allele (as is the case in heritable human retinoblastoma). The transgene was inherited with a mendelian pattern (50% of offspring receiving the transgene), indicating a single chromosomal integration site. To establish whether the transgene integrated into one allele of the *Rb* locus, the transgene was mapped on metaphase chromosomes by *in situ* hybridization using the *Tag* coding region as a probe. The mouse *Rb* gene has been mapped to chromosome 14 (refs 19 and 20); but, the *Tag* transgene was located at a single site on chromosome 4 between bands C5 and C7 (Fig. 3). It is also unlikely that the mouse retinoblastoma resulted from any other mutation in the *Rb* locus, because these animals had been bred to wild-type animals through 10 successive generations and the fully penetrant phenotype correlated 100% with the presence of the *Tag* transgene. In addition, because $p105^{Rb}$ is expressed ubiquitously[1,2], integration into this gene would not explain the specific expression of the transgene in the eye. The retinal-specific expression was probably a result of integration close to a transcriptional regulatory sequence capable of directing retinal-specific expression, such as an enhancer for a retinal-specific gene.

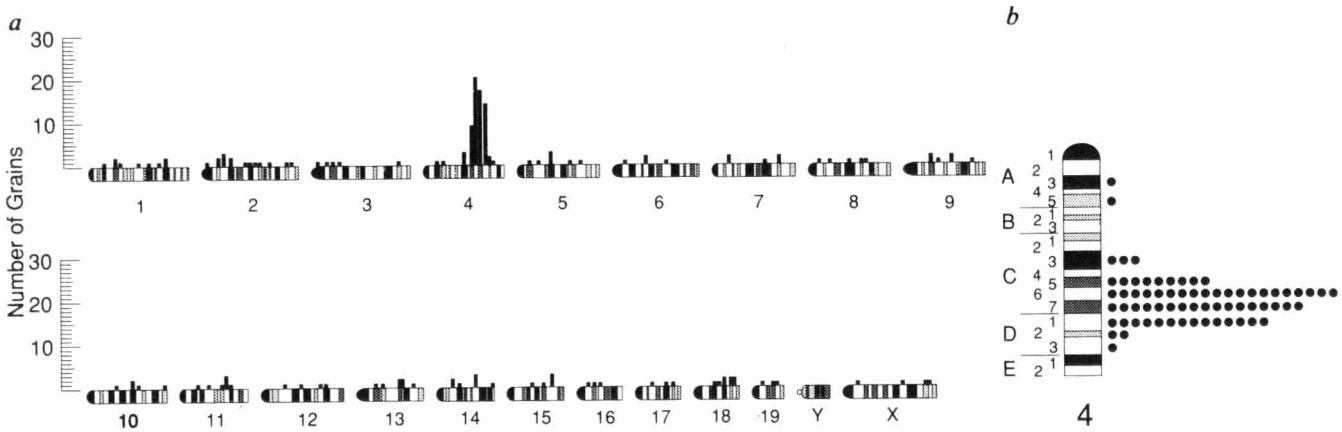

FIG. 3 Regional chromosome localization of the transgene. The plasmid SP6TagHB containing the *Tag* coding region of SV40 was labelled by nick translation using ^{3}H-labelled nucleotides to a specific activity of 6×10^{7} c.p.m. μg^{-1}. *In situ* hybridization to metaphase chromosomes from lymphocytes of a transgenic mouse was carried out using 0.02 μg per μl probe as described[35], and exposed for 7 days. A total of 81 metaphase cells were examined and chromosomes were identified by Q-band staining. *a*, Of 179 sites of hybridization scored, 65 (36% of the sites) were located between bands C3 and D2 of mouse chromosome 4. *b*, Each hybridization site on chromosome 4 often showed several grains indicating several copies of the transgene at the hybridization site. The largest number of sites were at bands C5–C7 (*b*). There was no significant hybridization to other chromosomes.

A more intriguing possibility for the ontogeny of tumorigenesis in these mice is indicated by the demonstrations of direct interactions between p105^{Rb} and T antigen[3] or other oncoproteins[21,22] in transformed fibroblasts or *in vitro*[22,23]. One mechanism by which T antigen could mediate tumorigenesis is through direct inhibition of the function of the Rb protein[24]. To demonstrate that both p105^{Rb} and Tag proteins were expressed, retinoblastoma cells were metabolically labelled with ^{32}P and protein extracts were immunoprecipitated with three antibodies: anti-mouse p105^{Rb} antiserum (Rb-138; ref. 25), anti-Tag antibody (PAb416; refs 3 and 26), and preimmune serum. Figure 4*a* demonstrates that the anti-mouse p105^{Rb} antiserum precipitated a protein of relative molecular mass 105,000 (M_r 105 K), whereas the anti-Tag antibody precipitated a 90K protein (TAG) and a 53K protein (presumed to be p53, another cellular oncoprotein that associates with Tag[27–29]). Both p105^{Rb} and Tag were therefore expressed in the murine retinoblastoma cells. From this experiment, it was difficult to assess whether p105^{Rb} and Tag were associated and could be co-immunoprecipitated, because a protein precipitated by both the preimmune serum and the anti-p105^{Rb} antiserum migrated to about the same position as Tag. In addition, p105^{Rb} would not be expected to be visible in the anti-Tag antibody lane, because Tag binds only the unphosphorylated form of p105^{Rb} (ref. 23), and these cells were labelled with ^{32}P. In order to demonstrate an association between p105^{Rb} and Tag, unlabelled extracts from ocular tumour cells were immunoprecipitated with anti-p105^{Rb} antiserum and analysed by western blotting using the anti-Tag antibody. Tag was co-immunoprecipitated by the anti-p105^{Rb} antiserum, indicating a direct interaction between p105^{Rb} and Tag (Fig. 4*b*). These observations strongly support a mechanism for the development of retinoblastoma in which the normal function of p105^{Rb} is impaired through binding to Tag specifically expressed in ocular tissues, and provide an

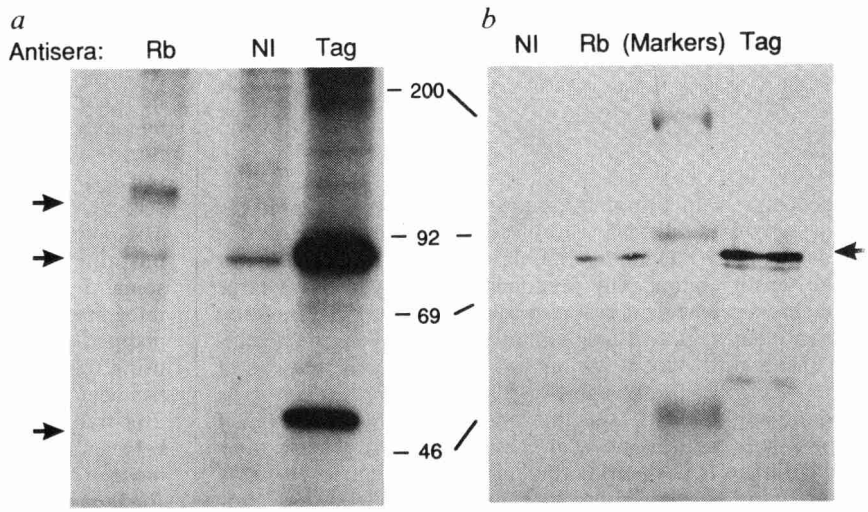

FIG. 4 Immunoprecipitation and western-blot analysis of Tag and p105^{Rb} from retinoblastoma tumour cells. *a*, Extracts from ^{32}P orthophosphate-labelled cultures of transgenic ocular tumours grown in nude mice were immunoprecipitated with a mouse monoclonal antibody to Tag (PAb-416; ref. 26), rabbit preimmune serum (138-NI; ref. 25), and a polyclonal antiserum directed against a portion of the murine p105^{Rb} (Rb-138; ref. 25). *b*, Unlabelled proteins extracted directly from transgenic ocular tumours were immunoprecipitated with the same three antisera and western-blotted with the antibody against Tag.

METHODS. *a*, About 10^{7} retinoblastoma cells from ocular transgenic tumours were introduced subcutaneously into nude mice. Nude mouse tumours were transferred to tissue culture and grown in DMEM, 15% horse serum and 5% fetal bovine serum. Retinoblastoma cells grew in suspension in characteristic clusters and any fibroblasts were removed due to adherence to plastic. Uniform populations of nonadherent cells were studied by light and electron microscopy and determined to be a pure population of retinoblastoma cells (data not shown). Cell cultures were treated with phosphate-free DMEM for 2 h at 37 °C and then labelled with 5 mCi of ^{32}P orthophosphate (NEN) in phosphate-free DMEM for 4 h at 37 °C. Cells were lysed in ELB buffer (0.15 M NaCl, 0.1% Nonidet P-40, 50 mM HEPES buffer, 1 mM phenylmethylsulphonyl fluoride, 5 mM EDTA, 0.5 mM dithiothreitol). Supernatants were precleared with protein A Sepharose, then incubated with appropriate antibodies for 8 h on ice. Proteins were immunoprecipitated with protein A Sepharose, washed with ELB buffer, and separated on a 7.5% SDS-polyacrylamide gel. *b*, Retinoblastoma cells from 10 ocular transgenic mouse tumours were dissected and lysed in ELB buffer. Nuclear proteins were precipitated and electrophoresed as described above, then transferred to nitrocellulose by electrophoresis. The filter was blocked by incubation in TBST (10 mM Tris–HCl buffer, pH 8.0, 150 mM NaCl, 0.05% Tween-20, 1% BSA) then incubated with 15 ml of a 1:100 dilution of PAb-416 for 1 h, washed in TBST and incubated with alkaline phosphatase-conjugated rabbit anti-mouse IgG (Promega). Colorimetric assays were performed according to the manufacturer's specifications.

explanation for the remarkable identity in morphology and malignant characteristics of the transgenic and human retinoblastomas.

Heritable retinoblastoma has greatly advanced our knowledge of the genetics of cancer. However, this malignancy has been observed exclusively in humans, and the absence of a heritable animal model has limited detailed understanding of the pathogenesis of this disease. We have described a line of transgenic mice that develop intraocular neoplasms with the histologic, ultrastructural, immunohistochemical and invasive features of human retinoblastoma, created by specific expression of the *Tag* oncogene in the retina. The demonstration that Tag interacts with the *Rb* anti-oncogene product, establishes that this association can occur in retinoblastoma tumours *in vivo* and provides strong evidence for its role in oncogenesis. This model provides an opportunity to study the process of malignant transformation in retinoblastoma *in vivo* from inception through extension and metastases. □

Received 6 November; accepted 13 December 1989.

1. Friend, S. H. *et al. Nature* **323,** 643–646 (1986).
2. Lee, W.-H. *et al. Science* **235,** 1394–1399 (1987).
3. DeCaprio, J. A. *et al. Cell* **54,** 275–283 (1988).
4. Talmadge, K., Vamvakopoulos, N. C. & Fiddes, J. C. *Nature* **307,** 37–40 (1984).
5. Brinster, R. L. *et al. Cell* **37,** 367–379 (1984).
6. Jenkins, N. A. & Copeland, N. G. in *Important Advances in Oncology* (eds DeVita, V. T., Hellum, S. & Rosenberg, S. A.) 61–77 (Lippincott, Philadelphia, 1989).
7. Hanahan, D. *Nature* **315,** 115–122 (1985).
8. Mahon, K. A. *et al. Science* **235,** 1622–1628 (1987).
9. Baetge, E. E., Behringer, R. R., Messing, A., Brinster, R. L. & Palmiter, R. D. *Proc. natn. Acad. Sci. U.S.A.* **85,** 3648–3652 (1988).
10. Botteri, F. M., van der Putten, H., Wong, D. F., Sauvage, C. A. & Evans, R. M. *Molec. cell. Biol.* **7,** 3178–3184 (1987).
11. Ts'o, M. O. M., Zimmerman, L. E. & Fine, B. S. *Am. J. Ophthal.* **69,** 339–349 (1970).
12. Ts'o, M. O. M., Fine, B. S. & Zimmerman, L. E. *Am. J. Ophthal.* **69,** 350–359 (1970).
13. Albert, D. M., Sang, D. N. & Craft, J. L. *Jap. J. Ophthal.* **22,** 358–374 (1978).
14. Flexner, S. *Bull. Johns Hopkins Hosp.* **2,** 115–119 (1891).
15. Wintersteiner, H. *Das Neuroepithelioma Retinae: Eine Anatomische und Klinische Studie* (Franz Deuticke, Vienna, 1887).
16. Wright, J. H. *J. exp. Med.* **12,** 556 (1910).
17. Kyritsis, A. P., Tsokos, M., Triche, T. J. & Chader, G. J. *Nature* **307,** 471–473 (1984).
18. Kivela, T. *Antigenic Properties of Retinoblastoma Tissue in Relation to Neuronal and Glial Cells of the Human Retina* 51–67 (University of Helsinki, 1987).
19. Stone, J. C. *et al. Genomics* **5,** 70–75 (1989).
20. Hsieh, C.-L. *et al. Somatic Cell molec. Genet.* **15,** 461–464 (1989).
21. Whyte, P. *et al. Nature* **334,** 124–129 (1988).
22. Dyson, N., Howley, P. M., Munger, K. & Harlow, E. *Science* **243,** 934–936 (1989).
23. Ludlow, J. W. *et al. Cell* **56,** 57–65 (1989).
24. Green, M. R. *Cell* **56,** 1–3 (1989).
25. Bernards, R. *et al. Proc. natn. Acad. Sci. U.S.A.* **86,** 6474–6478 (1989).
26. Harlow, E. *et al. J. Virol.* **39,** 861–869 (1981).
27. Lane, D. P. & Crawford, L. V. *Nature* **278,** 261–263 (1979).
28. Sarnow, P., Yo, Y., Williams, J. & Levine, A. J. *Cell* **28,** 387–394 (1982).
29. Efrat, S., Baekkeskov, S., Lane, D. & Hanahan, D. *EMBO J.* **6,** 2699–2704 (1987).
30. Chirgwin, J. M., Przybyla, A. E., MacDonald, R. J. & Rutter, W. J. *Biochemistry* **18,** 5294–5299 (1979).
31. Mellon, P. L., Parker, V., Gluzman, Y. & Maniatis, T. *Cell* **27,** 279–288 (1981).
32. Maniatis, T., Fritsch, E. F. & Sambrook, J. *Molecular Cloning: A Laboratory Manual* (Cold Spring Harbor Laboratory, New York, 1982).
33. Tooze, J. (ed.) *Molecular Biology of Tumor Viruses, Part 2* (Cold Spring Harbor Laboratory, New York, 1981).
34. Hogan, B., Costantini, F. & Lacy, E. *Manipulating the Mouse Embryo: A Laboratory Manual* (Cold Spring Harbor Laboratory, New York, 1986).
35. Tedder, T. F. *et al. J. Immun.* **141,** 4388–4394 (1988).

ACKNOWLEDGEMENTS. We thank R. Weiner and T. Dryja for discussions, and R. Davis for preliminary histological analysis. This work was supported by the NIH (P.L.M., D.M.A., J.M.O., D.M. and C.M.D.), the Edward J. Mallinckrodt Foundation and the Searle Scholarship Foundation (R.B.), the American Cancer Society and the J. Aron Charitable Foundation (J.J.W.) and the Massachusetts Lions Eye Research Fund (J.M.O. and D.M.)

Non-hydrophobic extracytoplasmic determinant of stop transfer in the prion protein

C. Spencer Yost*†, Charles D. Lopez†, Stanley B. Prusiner‡§, Richard M. Myers†§ & Vishwanath R. Lingappa†‖

Departments of * Anesthesia, † Physiology, ‡ Neurology, § Biochemistry and Biophysics, and ‖ Medicine, University of California, San Francisco, California 94143, USA

A UNIVERSAL feature of integral transmembrane proteins is a hydrophobic peptide segment that spans the lipid bilayer. These hydrophobic domains are important for terminating the translocation of the polypeptide chain across the membrane of the endoplasmic reticulum (a process termed stop transfer) and for integrating the protein into the bilayer[1–5]. But a role for extracytoplasmic sequences in stop transfer and transmembrane integration has not previously been shown. Recently, a sequence which directs an unusual mode of stop transfer has been identified in the prion protein. This brain glycoprotein exists in two isoforms[6–8], which are identical both in primary amino-acid sequence and in containing phosphatidylinositol glycolipid linkages at their C termini, which can be cleaved by a phophatidylinositol-specific phospholipase C[9]. But only one of the isoforms (PrP^C) is released from cells on treatment with this phospholipase[10], indicating that the two isoforms have either different subcellular locations or transmembrane orientations. Consistent with this is the observation of two different topological forms in cell-free systems[11,12]. An unusual topogenic sequence in the prion protein seems to direct these alternative topologies (manuscript in preparation). In the wheat-germ translation system, this sequence directs nascent chains to a transmembrane orientation; by contrast, in the rabbit reticulocyte lysate system, this sequence fails to cause stop transfer of most nascent chains. We have now investigated determinants in this unusual topogenic sequence that direct transmembrane topology, and have demonstrated that (1) a lumenally disposed charged domain is required for stop transfer at the adjacent hydrophobic domain, (2) a precise spatial relationship between these domains is essential for efficient stop transfer, and (3) codons encompassing this hydrophilic extracytoplasmic domain confer transmembrane topology to a heterologous protein when engineered adjacent to the codons for a normally translocated hydrophobic domain. These results identify an unexpected functional domain for stop transfer in the prion protein and have implications for the mechanism of membrane protein biogenesis.

We constructed a series of deletions throughout the prion protein (PrP) to demonstrate the significance of the unusual topogenic sequence. Figure 1 illustrates three of these mutants and compares them with the wild-type (wt) PrP molecule. We expressed these PrP mutants in the wheat-germ (WG) translation system supplemented with dog pancreas rough microsomal membranes. We digested aliquots with proteinase K in the presence or absence of the non-ionic detergent Triton X-100, and subjected them to SDS-PAGE. The protein encoded by the mutant PrP ha 32 (Fig. 2*a*, lanes 1–4) had the same topology as wt PrP (PrP ha 1; Fig. 2*b*, lanes 5–8), as determined by the size, intensity and proportion of the characteristic N-terminal transmembrane fragment generated on proteolysis of intact membranes (compare Fig. 2*b*, lanes 7 and 8 with Fig. 2*a*, lanes 3 and 4)[12]. Proteolysis in the presence of detergent completely hydrolysed translation products for PrP ha 32 and all other PrP mutants (Figs 2, 3 and 5). These results were as expected, in view of the large body of evidence indicating that only very discrete regions of a protein are involved in determining topology[13,14]. Indeed, deletion of other regions in the C-terminal end of PrP did not affect the transmembrane topology (data not shown).

PrP mutant ha 30 (Fig. 2*a*, lanes 5–8) which has deleted transmembrane regions has, as predicted, a fully translocated topology, as demonstrated by glycosylation and protection from protease digestion in the absence of detergents. This is consistent with previous studies demonstrating an absolute requirement for the hydrophobic domain in transmembrane integration[1,2,15].

The gene encoding the mutant PrP ha 28 (Fig. 1) has a deletion of 24 codons just 5′ to the region encoding the first transmembrane region, but leaves the entire transmembrane region